Available online at www.sciencedirect.com

ScienceDirect

IFAC Papers Online CONFERENCE PAPER ARCHIVE

IFAC PapersOnLine 56-3 (2023) 127–132

Robust Estimation of State of Charge in Lithium Iron Phosphate Cells Enabled by Online Parameter Estimation and Deep Neural Networks

Junzhe Shi * **Dylan Kato** ** **Shida Jiang** ***
Chitra Dangwal **** **Scott Moura** †

* *University of California Berkeley, Berkeley , CA 94703 USA (e-mail: junzhe@berekeley.edu).*
** *University of California Berkeley, Berkeley , CA 94703 USA (e-mail: dkkato@berekeley.edu).*
*** *University of California Berkeley, Berkeley , CA 94703 USA (e-mail: shida_jiang@berekeley.edu).*
**** *University of California Berkeley, Berkeley , CA 94703 USA (e-mail: dangwal@berekeley.edu).*
† *University of California Berkeley, Berkeley , CA 94703 USA (e-mail: @berekeley.edu).*

Abstract: This paper addresses the state of charge estimation problem in lithium iron phosphate (LFP) battery cells. LFP cells are particularly challenging because their flat open circuit voltage (OCV) curve means OCV-based battery models are weakly observable. This means standard methods for SOC estimation don't easily converge to the true SOC. Additionally, in practice, estimates must be accurate in the face of biased noise on current input, as well as mean-zero noise on measurements. As such, we aim to create an estimator that is accurate when facing these types of noise. We accomplish this with a three-layer estimation technique that uses an adaptive Kalman filter, a Neural Network, and a Kalman Filter to estimate the state of charge. This method achieves an SOC estimation with an RMSE of 2.248%, even in the presence of a 0.2A current measurement bias and 5mA and 5mV random measurement noise. Notably, the proposed approach outperforms state-of-the-art methods like the extended Kalman filter.

Keywords: Energy systems, State of Charge Estimation, Lithium Iron Phosphate, Neural Network, Kalman filter, Parameter and state estimation, Energy Storage

1. INTRODUCTION

1.1 Problem setting/motivation

Batteries are a key enabling technology for a number of systems like electric vehicles, grid energy storage, and personal devices. One battery chemistry that is gaining growing attention is lithium iron phosphate (LFP) batteries. This chemistry has a number of strengths, the foremost of which are its low cost, safety, and high cycle life. However, state of charge (SOC) estimation is particularly difficult with this chemistry. This is because the middle SOC region has a particularly weak relationship between SOC and open circuit voltage (OCV). The "flat OCV" curve means that the SOC has little effect on the measured voltage in the middle SOC ranges. This motivates us to look for new estimation techniques that are less reliant on the OCV relationship.

1.2 Literature Review

There is a wide range of techniques for SOC estimation that have been well-studied for Lithium-ion batteries. Waag et al. (2014) and Li et al. (2017) provide a comprehensive review of state-of-the-art SOC estimation algorithms. Of particular interest in this paper are Kalman filtering techniques and Neural Network approaches. Kalman filtering techniques are pervasive in battery modeling due largely to their ease of implementation, theoretical guarantees in some cases, and reliability. Hossain et al. (2022) provide an overview of these techniques for SOC estimation.

More recently, neural network based approaches have also seen success for SOC estimation (Lipu et al. (2022); Liu et al. (2022)). Because neural networks act as general function approximators, they are able to capture complex dynamics present in the data that are difficult to model

⋆ This material is based upon work supported by the National Science Foundation Graduate Research Fellowship Program under Grant No. DGE 2146752 and Grant No. 1847177. Any opinions, findings, and conclusions or recommendations expressed in this material are those of the author(s) and do not necessarily reflect the views of the National Science Foundation. This work is also partially supported by TotalEnergies/Saft under Award No. 20163367.

10.1016/j.ifacol.2023.12.012

with traditional battery models. The downside of these approaches is they usually struggle with out-of-sample performance and sometimes require large amounts of data. Some approaches like those presented in Charkhgard and Farrokhi (2010) have combined Kalman filtering with neural network approaches. Such hybrid estimation methods have the potential to leverage the strengths of both techniques.

While these state of art SOC estimation techniques perform well on chemistries like nickel manganese cobalt (NMC), they struggle when applied to LFP cells. The key challenge in LFP cells is the flat OCV curve (see 1), which makes the system weakly observable. Weak observability makes LFP SOC estimation vulnerable to sensor and process noise. Li et al. (2013) compares 3 SOC estimators: Luenberger observer, extended Kalman filter (EKF), and sigma-point Kalman filter (SPKF) for an LFP pouch cell. Different neural network based methods for LFP estimation have also been explored. Chang (2016) uses fuzzy neural networks and compares the results to backpropagation NN and Coulomb counting. Huawei et al. (2019) compares radial basis function NN to backpropagation NN for LFP SOC estimation in terms of the tradeoff between accuracy and time efficiency. Chen et al. (2022) uses a deep neural network (DNN) to obtain a SOC estimate which they then filter with a Kalman filter. There has also been some work with hybrid estimation techniques that exploit charging protocols to train the DNN. The DNN is then used for estimating accurate initial SOC for Coulomb counting (Tian et al. (2021); Hu et al. (2022)). While many of these techniques show promising results, all of these works are done assuming no current sensor bias. Though they are able to obtain good results, the results are collected from laboratory equipment using high-accuracy voltage and current measurement sensors and with correct initial conditions on SOC. Such assumptions mean the results do not generalize to real-world applications, which are subject to corruption by noise on both voltage and current measurements.

Some work has examined estimation in the presence of sensor bias. For example, Lin (2018) presents theoretical estimation bounds of recursive observers with output error injection to input bias. Other works develop specific estimation algorithms that explicitly estimate current bias, in order to obtain more accurate estimates Shen et al. (2021); Feng et al. (2017); He et al. (2019). These works focus on NMC chemistries, however, and therefore rely on the strong OCV relationship to estimate bias.

A clear gap in the LFP SOC estimation literature is robustness to input bias. Input bias can arise from a number of different sources, including uncertainty of current distribution in packs, Coulombic losses, or faulty sensors. As such, it is important to develop techniques for effectively estimating SOC in the face of current bias. To address the challenges of LFP SOC estimation, especially when dealing with sensor noise and bias, we propose a robust SOC estimation technique that combines online parameter identification with a hybrid DNN and KF state estimator.

1.3 Contributions

The key contribution of work are:

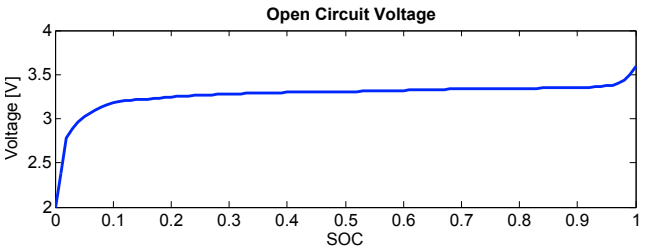

Fig. 1. OCV as function of SOC for an LFP cell. Note that OCV is nearly flat from 15% - 95% SOC, increasing by less than 2mV per 1% SOC change on average.

(1) A novel approach to SOC estimation in LFP battery cells that trains a neural network on parameter estimates generated from a Kalman filter.
(2) Accurate SOC estimates in a model to model study in the face of current bias and voltage noise.
(3) Accurate SOC estimates demonstrated for prolonged cycling in the flat-OCV region.
(4) Demonstration that this novel estimation algorithm outperforms other state of art benchmark methods.

2. METHODS

2.1 General Structure of the SOC Estimator

As shown in Fig. 2, the proposed method consists of two main parts: offline training and online estimation. In the offline training, a training set is constructed based on current and terminal voltage data from selected training profiles. These profiles provide voltage and current data with accurate battery SOC values, obtained by simulating an LFP cell with various current profiles cycles. Using these profiles, the battery parameters are identified using a parameter estimation KF. The identified battery parameters and SOC data are used to train a DNN that predicts battery SOC using two selected battery parameters, OCV and α. The significance of α is elaborated upon in Section 2.2. After training is complete, the DNN is tested on a validation set, and the estimation variance is calculated. In the online estimation, real-time terminal voltage and current data are fed into the parameter estimation KF, which provides the online identified OCV and α values to the DNN. These parameter estimates are fed into the DNN which ouputs an SOC estimate, as shown in Fig. 2. The final estimation is made by synthesizing the coulomb counting value and DNN estimation results, using a data fusion KF that minimizes the variance. The detailed algorithms used in each part are introduced in the following subsections.

2.2 Kalman Filter for Parameter Estimation

A Kalman filter is comprised of two steps, namely the prediction and the measurement update. The KF equations are presented below,

Step 1: Prediction:

$$x_p(k) = A(k-1)x_m(k-1) + B(k-1)u(k-1) \quad (1)$$

$$P_p(k) = A(k-1)P_m(k-1)A(k-1)^T + \Sigma_{vv}(k) \quad (2)$$

Step 2: Measurement update:

$$K(k) = P_p(k)H(k)^T(H(k)P_p(k)H(k)^T + \Sigma_{ww}(k))^{-1} \quad (3)$$

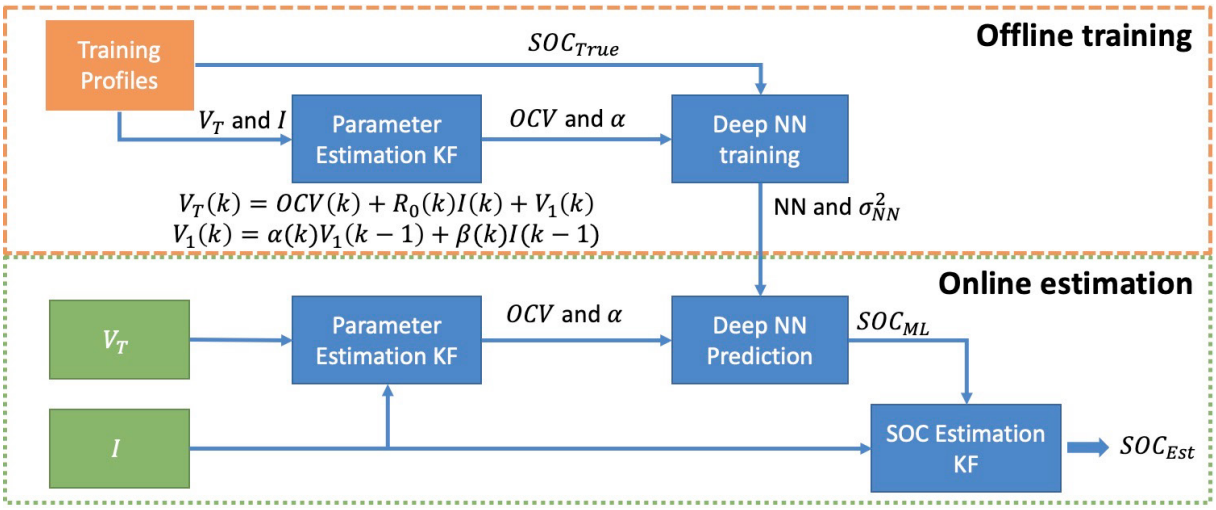

Fig. 2. A block diagram of the proposed method.

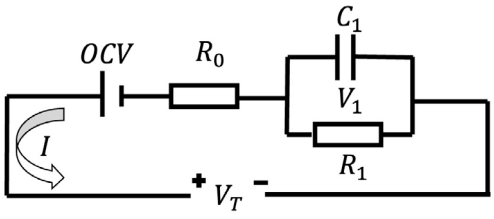

Fig. 3. The battery 1RC equivalent circuit model used in this paper.

$$x_m(k) = x_p(k) + K(z(k) - H(k)x_p(k)) \quad (4)$$

$$P_m(k) = (I - K(k)H(k))P_p(k) \quad (5)$$

where x represents the states of the system, u is the input, z is the measurement. A is the state-transition matrix, which describes how the state of the system evolves over time. B is the input matrix, which relates the input to the state of the system. H the observation matrix, which maps the state of the system to the measurements obtained from the system. P is the covariance matrix of the states, $\boldsymbol{I}$ is the identity matrix, K is the Kalman gain, Σ_{ww} is the covariance matrix of the process noise, and Σ_{vv} is the variance of the measurement.

To develop the KF for estimating the parameters we first define our battery model. The battery model used in the KF is an equivalent circuit model (ECM), illustrated in Fig. 3. This model is comprised of a voltage source (OCV), an internal resistance (R_0), and an RC pair (R_1 and C_1). It is conventional to treat OCV as a function of the SOC. However, for our method we will treat OCV as a time varying parameter. Hence we only need to model the dynamics of the voltage across the RC pair. These are given by:

$$V_1(k) = V_1(k-1)\alpha(k) + I(k-1)\beta(k) \quad (6)$$

Here, $\alpha = \exp(-\Delta t/(R_1C_1))$, and $\beta = R_1(1-\alpha)$. The output of the model is the terminal voltage V_T and is given by the sum of the open circuit voltage, IR drop, and capacitor voltage:

$$V_T(k) = OCV(k) + R_0(k)I(k) + V_1(k) \quad (7)$$

According to the battery model, the parameters OCV, R_0, α, and β, are selected as the KF states. The discrete state transition function and measurement function of the model can be written as follows.

$$\boldsymbol{x}(k) = \begin{bmatrix} OCV(k) \\ R_0(k) \\ \alpha(k) \\ \beta(k) \end{bmatrix} \quad (8)$$

$$x(k) = x(k-1) + v \quad (9)$$

$$V_T(k) = y(k) = Hx(k) + w \quad (10)$$

where v and w are the process and measurement noise, respectively, and

$$H = [1,\ I(k),\ V_1(k-1),\ I(k-1)] \quad (11)$$

Using the above x, H, y and the measured voltage as z we use equations (1)-(5) to estimate $x(k)$. This comes with one caveat. Since we need $V_1(k-1)$ to express H we also compute this value according to equation (6). This update occurs after the prediction update but before the measurement update in the Kalman filter.

2.3 Training the DNN for SOC Estimation

The DNN used in this paper is a three-layer, fully connected NN with twenty hidden units in each layer. Rectified linear unit (ReLU) activation functions were used in the hidden layers of the deep neural network. The inputs of the DNN are OCV and α, estimated by the parameter estimation KF. Note that only two states (OCV, α) instead of four states (OCV, R_0, α, β) are used as the inputs. Equation (11) indicates that the estimated parameters R_0 and β are sensitive to current measurement. Excluding them from the inputs can improve the method's robustness to the noise and bias in current measurements, which is a significant advantage of the proposed method.

For efficient training and evaluation of our machine learning model, we partitioned our data resources into three distinct subsets: the training set, the validation set, and the test set. Data for model training and validation were sourced from the same collection, which comprised six

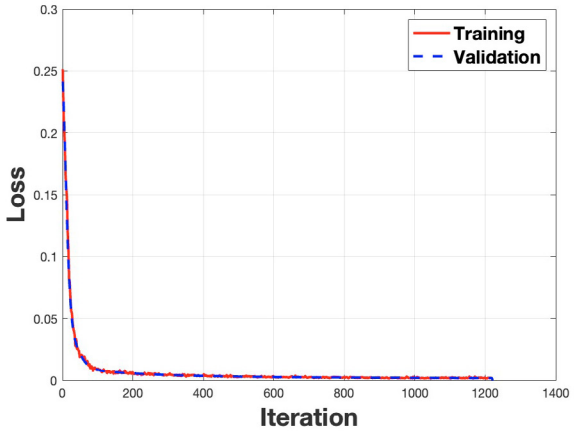

Fig. 4. Learning Curve: Training and Validation Loss over Iterations.

real-world driving cycles including UDDS, US06, New York City Cycle, etc., obtained from NREL (2023). We allocated 70% of this dataset to the training process. The remaining 30% served as the validation set, playing a crucial role in tuning the model's parameters and informing significant decisions throughout the training phase. In contrast, to assess our model's capacity to adapt to new scenarios, we employed an independent test set derived from a separate source: the Orange County Transit Bus Cycle (US-OCTA). The training, validation, and test datasets for the proposed method were generated by charging and discharging an LFP cell model, as described in Lin et al. (2014). The SOC data were meticulously recorded during these charging and discharging processes. To bolster the proposed DNN's resilience to current fluctuations and measurement noise, artificial measurement noises were integrated into the training and validation data.

Upon estimating the battery parameters OCV and α using the parameter estimation Kalman filter, these were utilized in tandem with the true SOC data to train the DNN, $f_{DNN}(OCV, \alpha)$, to predict battery SOC. It's worth noting that the training data and estimation parameters, particularly OCV, derived from the parameter Estimation KF, closely align with the actual parameters of the model used in the simulation. The primary objective is to discover an optimal method that enables the DNN to balance the estimation based on the OCV and α values. Hence, the proposed DNN is designed to estimate the battery SOC using Equation (12). Furthermore, the mean-square error of SOC prediction using the validation set, represented by σ^2_{NN}, was recorded for future use in online estimation.

$$SOC_{ML}(k) = f_{DNN}(OCV(k), \alpha(k)) \tag{12}$$

As shown in Fig. 4, the model demonstrated low loss values in both the training and validation sets. This low loss value is indicative of a small difference between the model's predicted SOC values and the actual SOC values in our training and validation data, suggesting accuracy in SOC prediction without over fitting and under fitting.

2.4 Kalman filter for SOC synthesis

While coulomb counting is a straightforward method for estimating the SOC by integrating the current over time, its accuracy can be compromised by an inaccurate initial guess of SOC and noise and bias in the current measurement. To address these challenges, this study proposes a SOC estimation Kalman filter to fuse the SOC estimations made by both the coulomb counting and DNN methods. In this approach, the DNN serves as the measurement source for the SOC estimation KF in the measurement update step, while the coulomb counting method acts as the model for updating the SOC in the prediction step.

The dynamical system we will use for SOC estimation tracks the state of charge i.e. $x(k) = SOC(k)$. We chose to advance the dynamics of the estimate using coulomb counting so $A = 1$ and we have $H = 1$ so that the output, y, is the SOC estimate. The dynamics of the system with process and measurement noise v and w are then given by the following equations.

$$x(k) = x(k-1) + \frac{I(k-1)\Delta t}{Q_{cap}} + v \tag{13}$$

$$y(k) = x(k) + w \tag{14}$$

where Q_{cap} is the capacity of the LFP cell, and Δt is the sampling time of the system. Further, we use the output of the deep neural network as our measurement namely:

$$z(k) = SOC_{ML}(k) = f_{DNN}(OCV(k), \alpha(k)) \tag{15}$$

Using the above x, A, H and z we implement (1)-(5). giving the following equations:

$$SOC_p(k) = SOC_m(k-1) + \frac{I(k-1)\Delta t}{Q_{cap}} \tag{16}$$

$$P_p(k) = P_m(k-1) + \Sigma_{vv}(k) \tag{17}$$

$$K(k) = \frac{P_p(k)}{P_p(k) + \Sigma_{ww}(k)} \tag{18}$$

$$SOC_m(k) = (1 - K(k))SOC_p(k) + K(k)(SOC_{ML}(k)) \tag{19}$$

$$P_m(k) = (1 - K(k))P_p(k) \tag{20}$$

This method hybridizes the coulomb counting method with the estimates from the DNN. Coulomb counting is prone to inaccuracies in the initial guess of SOC and noise and bias in the current measurement. DNN estimation error, as shown in figure 5 is prone to noise ,as seen in the blue curve. By leveraging the advantages of both coulomb counting and the DNN, the proposed method provides a relatively accurate and smooth SOC estimation, even when the measurement is noisy and biased and the OCV curve is flat.

3. PERFORMANCE AND DISCUSSION

3.1 Test Overview

The performance of the proposed algorithm was assessed through a test cycle under a flat OCV range, spanning from 90% to 20% SOC. To emulate real-world electric vehicle operation, the test employed the US-OCTA Cycle. To benchmark the proposed method, pure machine learning (ML) and EKF methods were used. Additionally, to demonstrate the algorithm's robustness, different current biases, and random measurement noises were introduced into the current and voltage measurements. These random

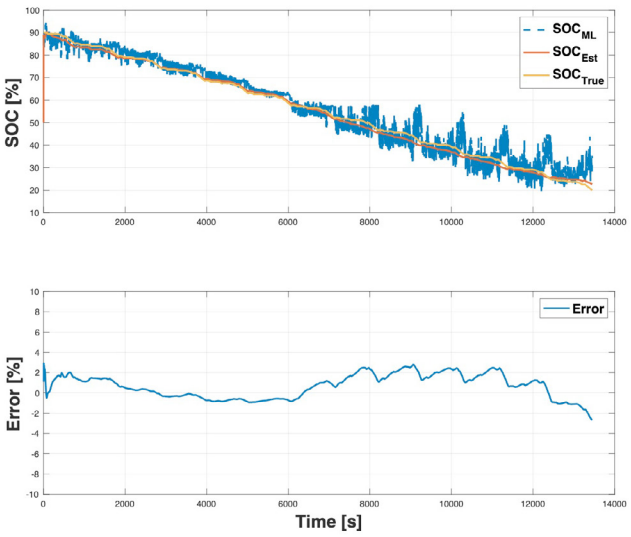

Fig. 5. SOC estimation results of the proposed method with 0.1A current measurement bias and 5mA and 5 mV random measurement noises.

noises follow normal distributions with standard deviations of 5mA for current and 5mV for voltage measurements. Moreover, the initial guessed SOC of the proposed method and EKF was set to 50%, corresponding to a 40% initial error for testing purposes.

3.2 Estimator Performance for an Extended Drive Cycle

Figure 5 presents the SOC estimation results obtained using the proposed method, taking into account a 0.1A current measurement bias and 5mA and 5mV random measurement noises. The blue dashed line represents the SOC values obtained from the DNN, while the red line shows the final estimated SOC results generated by combining the DNN and coulomb counting outcomes using KF. The yellow line denotes the true SOC data. Note the true SOC curve generally tracks the average of the DNN prediction results, indicating the DNN has some robustness to measurement bias. In the SOC estimation KF, the DNN's output plays the role of output measurement. Since the DNN's estimate is nearly zero-mean (albeit with some noise), it can be fed into a Kalman filter. In other words, the SOC_{ML} results correct the Coulomb counting estimate, which is erroneous due to (i) incorrect initial SOC, and (ii) biased current measurements. Consequently, the SOC estimation converges near the true SOC within a few time steps. Leveraging the coulomb counting method, the online SOC estimation KF produces smooth SOC estimation results even in the presence of current and voltage noise. Additionally, the DNN results can promptly correct the impact of any current bias on the coulomb counting. As a result, the proposed method shows promising results against both measurement noise and bias, with an RMSE of only 2.0825% in the test case.

3.3 Robustness to Different Current Biases

The SOC estimation result obtained using the proposed method is compared against two benchmarks: the EKF method and a pure ML method. We compare the true SOC values with the estimates of each method in Fig. 6. The methods are evaluated with four different current biases, ranging from -0.2A to 0.2A, and with 5mA and 5mV random measurement noises. The results show that the proposed method provides more consistent SOC estimation results, and is the least impacted by high current biases, as demonstrated in the first subplot in Fig. 6.

The second subplot in Fig. 6 shows the EKF results, which utilizes a two RC equivalent circuit model fitted with true battery data. Due to the relatively high initial error, the EKF method employs a larger initial variance. To correct the estimation, the measurement updates are given more weight, leading to an initial jump in the estimated SOC toward the true SOC. However, the EKF method does not handle measurement noise and bias well, resulting in poor performance. The method is highly sensitive to measurement noise in the flat OCV zone due to high observer gain. Also, the current bias leads to accumulated model update errors, yielding a divergent drift in the SOC estimates.

The pure ML method, shown in the third subplot in Fig. 6, utilizes a DNN with 100 sequential voltage and current data as inputs. Since the current and voltage noise and current bias are directly fed into the pure ML model, the method is sensitive to noise and bias. As shown in Fig. 6, measurement noise leads to noisy SOC estimates. Meanwhile, biased current measurements cause the SOC estimates to drift away from the true SOC values.

The RMSE for each method under different current biases is reported in Table 1. Overall, the simulations demonstrate the robustness and effectiveness of the proposed method in dealing with the flat OCV range. Upon examining the fitted parameters for LFP cells, it becomes evident that not only does the OCV change with SOC, but other parameters such as R_0, R_1, and C_1 also vary with SOC. Exploiting this parameter-SOC dependence may be valuable for estimating SOC. In our proposed method, note that the DNN predicts SOC as a function of both SOC and $\alpha = \exp(-\Delta t/(R_1 C_1))$. Thus, the introduction of α contributes valuable information regarding SOC, especially in the flat OCV range. The proposed method is also robust to current biases by relying on estimated parameters that are insensitive to current measurements.

3.4 Discussion of drawbacks

Besides the advantages of the proposed method, the method also has a drawback/limitation in that it requires an input current profile that provides sufficient excitation. Because the proposed method utilizes online parameter estimation to obtain OCV and α values, the proposed method does not work well when the input current is constant for an extended period of time. The online parameter estimation requires a varying input current to ensure sufficient excitation for accurate parameter estimation.

4. CONCLUSION

In this study, we proposed a novel hybrid method for online SOC estimation of LFP batteries, which integrates machine learning and Kalman filtering techniques. The

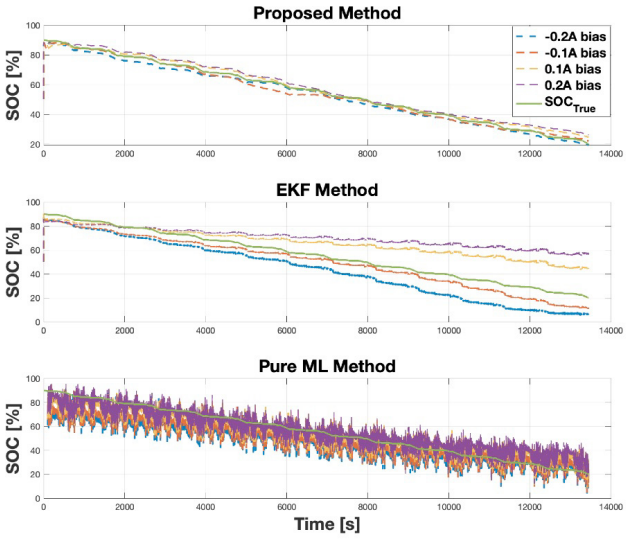

Fig. 6. SOC estimation results using the pure ML and EKF methods.

method was validated in a model-to-model setting, and its performance was benchmarked against both a pure machine learning approach and an extended Kalman filter. Our findings demonstrate that the proposed method delivers superior SOC estimation accuracy, even amid high measurement noise and test case bias. Notably, the training profiles utilized in the study are used to provide sufficient excitation, enabling the neural network model to learn the nonlinear relationship between the battery's parameters and its SOC. Tailoring the design of training profiles could potentially boost the performance of the proposed method and decrease the volume of training data required. Therefore, future research could concentrate on the design of training profiles.

REFERENCES

Chang, W.Y. (2016). State of charge estimation for lfp battery using fuzzy neural network. *International Journal of Electrical and Electronics Engineering Research (IJEEER)*, 6(5), 25–32.

Charkhgard, M. and Farrokhi, M. (2010). State-of-charge estimation for lithium-ion batteries using neural networks and ekf. *IEEE transactions on industrial electronics*, 57(12), 4178–4187.

Chen, G., Jiang, S., Xie, M., and Yang, F. (2022). A hybrid dnn-kf model for real-time soc estimation of lithium-ion batteries under different ambient temperatures. In *2022 Global Reliability and Prognostics and Health Management (PHM-Yantai)*, 1–5. IEEE.

Feng, D., Huang, D., and He, J. (2017). Offset-free ecm based soc estimation using h-infinity observer. In *2017 IEEE International Conference on Mechatronics and Automation (ICMA)*, 76–80. IEEE.

Table 1. RMSE (%) with different current measurement biases

	-0.2A	-0.1A	0.1A	0.2A
Proposed Method	3.826%	2.243%	2.082%	2.248%
EKF	19.381%	13.611%	5.764%	12.598%
Pure ML	7.177%	7.136%	9.073%	10.535%

He, J., Feng, D., Hu, C., Wei, Z., and Yan, F. (2019). Two-layer online state-of-charge estimation of lithium-ion battery with current sensor bias correction. *International Journal of Energy Research*, 43(8), 3837–3852.

Hossain, M., Haque, M., and Arif, M.T. (2022). Kalman filtering techniques for the online model parameters and state of charge estimation of the li-ion batteries: A comparative analysis. *Journal of Energy Storage*, 51, 104174.

Hu, C., Ma, L., Guo, S., Guo, G., and Han, Z. (2022). Deep learning enabled state-of-charge estimation of lifepo4 batteries: A systematic validation on state-of-the-art charging protocols. *Energy*, 246, 123404.

Huawei, W., Yuanjin, Z., and Congjin, Y. (2019). Estimation of power battery soc based on firefly bp neural network. *Energy Storage Science and Technology*, 8(3), 575.

Li, J., Barillas, J.K., Guenther, C., and Danzer, M.A. (2013). A comparative study of state of charge estimation algorithms for lifepo4 batteries used in electric vehicles. *Journal of power sources*, 230, 244–250.

Li, Z., Huang, J., Liaw, B.Y., and Zhang, J. (2017). On state-of-charge determination for lithium-ion batteries. *Journal of Power Sources*, 348, 281–301.

Lin, X. (2018). Theoretical analysis of battery soc estimation errors under sensor bias and variance. *IEEE Transactions on Industrial Electronics*, 65(9), 7138–7148.

Lin, X., Perez, H.E., Mohan, S., Siegel, J.B., Stefanopoulou, A.G., Ding, Y., and Castanier, M.P. (2014). A lumped-parameter electro-thermal model for cylindrical batteries. *Journal of Power Sources*, 257, 1–11.

Lipu, M.H., Ansari, S., Miah, M.S., Meraj, S.T., Hasan, K., Shihavuddin, A., Hannan, M., Muttaqi, K.M., and Hussain, A. (2022). Deep learning enabled state of charge, state of health and remaining useful life estimation for smart battery management system: Methods, implementations, issues and prospects. *Journal of Energy Storage*, 55, 105752.

Liu, Y., He, Y., Bian, H., Guo, W., and Zhang, X. (2022). A review of lithium-ion battery state of charge estimation based on deep learning: Directions for improvement and future trends. *Journal of Energy Storage*, 52, 104664.

NREL (2023). Drivecat - chassis dynamometer drive cycles. *National Renewabel Energy Laboratory*, www.nrel.gov/transportation/drive-cycle-tool.

Shen, J., Wang, Q., Zhao, G., Ma, Z., and He, Y. (2021). A joint moving horizon strategy for state-of-charge estimation of lithium-ion batteries under combined measurement uncertainty. *Journal of Energy Storage*, 44, 103316.

Tian, J., Xiong, R., Shen, W., and Lu, J. (2021). State-of-charge estimation of lifepo4 batteries in electric vehicles: A deep-learning enabled approach. *Applied Energy*, 291, 116812.

Waag, W., Fleischer, C., and Sauer, D.U. (2014). Critical review of the methods for monitoring of lithium-ion batteries in electric and hybrid vehicles. *Journal of Power Sources*, 258, 321–339.